MIXED CONVECTION BETWEEN HORIZONTAL PARALLEL PLATES

الحمـــل المختلط بين لوحين افقـيين متـــوازيين

M. MAHGOUB, M. G. WASEL, M. S. GHITH
Mechanical Power Eng., Faculty of Engineering,
Mansoura University, Mansoura, Egypt

ملخص :

في هذا البحث تم دراسة خصائص السريان الرقـائقي بـالحمل المختلط فـي منطقة المدخل بين لوحين أفقيين متوازيين معرضين لحالات مختلفة مـن التسـخين بثبوت درجـة الحرارة. لقد أمكن تحويل المعادلات الواصفة للسريان (كل من معادلتي الحركة في الاتجاه الطولي والعمودي عليـه مـع معادلـة الطاقـة) الـى صـورة لابعدية بادخال متغيرات مستقلة وتابعة جديدة في صورة لابعدية مناسبة. كمـا تـم تعريـف درجـة الحـرارة اللابعدية فـي صورة جديدة تحقق الشروط الحدية في حالات التسخين المختلفة.

استخدمت طريقة الحلول المحلية التشابهية في معالجة المعادلات في صـورتها اللابعدية الجديدة وباستخدام هذه الطريقة فان المعادلات اللابعدية للحركة والطاقة قد أمكن تبسيطها الى مجموعة من المعـادلات التفاضلية العاديـة الاتية التي استخدمت طريقة رونج-كوتا متبوعة بطريقة الرصد لحلها محليا عند قطاعات مختلفـة فـي الاتجـاه الطولي مع تحقيق الحالات الحدية في حالات التسخين المحتلفة. تم الحصـول علـى نتـائج لكل مـن معامل انتقال الحرارة، معامل الاحتكاك، كذلك توزيعات السرعة ودرجة الحرارة. كما تـم بحث تـأثير كل مـن معـامل الحمل المختلط ومعامل الشكل ورقم براندتل وكذلك النسبة بين درجتي حرارة السـطحين علـى كل مـن رقـم نوسـلت ومعامل الاحتكاك.

تبين من النتائج حدوث زيادة مضطردة في كل مـن رقـم نوسلت ومعـامل الاحتكـاك مـع زيـادة معـامل الحمل المختلط. أظهرت النتائج أيضـا أن لمعامل الشكل تأثيرا مخالفا لتأثير معامل الحمل المختلط. فزيادة معامل الشكل تؤدى الى نقص رقم نوسلت ومعامل الاحتكاك. أما بالنسبة لمنحنيات توزيع السرعة ودرجات الحرارة فـي جميع حالات التسخين، فقد أظهرت تغيرا ملحوظا عن نتائج الدراسات السابقة لحالة الحمل الجبرى.

ABSTRACT

In the present study laminar mixed convection between two horizontal parallel plates kept at symmetric and asymmetric uniform wall temperatures is studied . The momentum and energy equations are transformed to a dimensionless form by introducing appropriate dependent and independent variables and a dimensionless temperature ratio. The local similarity solution method is implemented to transform the governing equations to a system of ordinary differential equations. The locally similar equations are solved numerically by the Runge-Kutta integration technique along with the Newton-Raphson shooting method at different axial locations over the range of the mixed convection parameter $0.015 \leq \xi \leq 0.1$. Results are obtained for the local heat transfer, coefficient of friction, and velocity and temperature distributions. Effects of the mixed convection parameter, the configuration parameter, Prandtl number and the temperature ratio are studied.

NOMENCLATURE

b	vertical distance between the lower and upper plates
C_f	dimensionless coefficient of friction, $\tau_w / \rho u_o^2$
f	dimensionless stream function, $\psi / \sqrt{u_o \nu x}$
g	gravitational acceleration
Gr_b	Grashof number defined as, $g\beta(T_l - T_o)b^3/\nu^2$
Gr_x	Grashof number defined as, $g\beta(T_l - T_o)x^3/\nu^2$
h	local heat transfer coefficient
k	coefficient of thermal conductivity
Nu	local Nusselt number based on x, hx/k
Nu_b	local Nusselt number defined as, hb/k
P	pressure
Pr	Prandtl number, ν/α
q_w	heat flux at the wall
Re_b	Reynolds number defined as, $u_o b/\nu$
Re_x	Reynolds number defined as, $u_o x/\nu$
T	temperature
T_l	temperature of the lower plate
T_o	temperature of the fluid at the axis of the passage
Tr	dimensionless temperature ratio , $(2\phi+1)\phi/(2+\phi)$
T_u	temperature of the upper plate
u	velocity component in the longitudinal direction
u_o	free stream velocity at the inlet
v	velocity component in the normal direction
x	co-ordinate in the longitudinal direction
y	co-ordinate normal to the longitudinal direction
α	coefficient of thermal diffusivity
β	coefficient of thermal expansion
η	dimensionless independent variable, $y\sqrt{u_o/\nu x}$
η_{max}	the value of the independent variable η at the axis of the passage (i.e. at y=b/2)
ξ	mixed convection parameter, $Gr_x / Re_x^{5/2}$
ξ_b	configuration parameter, $Gr_b / 2Re_b^2$
ϕ	the temperature ratio between the two plates, $(T_l - T_o)/(T_u - T_o)$
ν	kinematic viscosity
ρ	density
ϑ	dimensionless temperature, $(T-T_o)/(T_l - T_o).Tr$
τ_w	wall shear stress, $\nu\rho(\partial u/\partial y)_w$
ψ	stream function, $f\sqrt{u_o \nu x}$

Introduction

The phenomenon of mixed convective heat transfer in the combined entrance region in various duct geometeries becomes increasingly important as the volume of the thermal devices are made smaller. The increasing use of such devices in the modern technology has stimulated continuing interest of many investigators in the recent years. Cheng and Whang [1] studied the laminar combined free and forced convection in horizontal rectangular channels under the thermal boundary conditions of axially uniform wall heat flux and peripherally uniform wall temperature for Various aspect ratios using a finite difference scheme.

Whang and Cheng [2] numerically determined the conditions marking the onset of longitudinal vortex rolls due to buoyant forces in the thermal entrance region of a horizontal parallel plate channel heated from below and cooled from above.

Wuu-ou, Cheng and Lin [3] studied the combined free and forced laminar convection with an upward flow in inclined rectangular channels having different aspect ratios using a modified formulation for the Reynolds and Rayliegh numbers, by which the inclination angle did not appear explicitly in the governing equations.

Abou-Ellail and Morcos [4] studied numerically buoyancy effects in the thermal entrance region of horizontal rectangular channels by transforming Navier-Stokes equations to a parabolic nature . A combined iterative-marching integration technique is employed to solve the finite difference equations.

Kennedy and Zebib [5] performed numerical and experimental studies to investigate the heat transfer characteristics and flow patterns resulting from four specific local heat source configurations located in four different ways so that the effect of the bottom heating only, the top heating only and the top and bottom heating could be investigated. Results are obtained for Reynolds numbers of 37 and Grashof numbers of 1.8×10^5 and 5.4×10^5.

Osborne and Incropera [6] conducted experimental study to investigate the hydrodynamic and thermal conditions in laminar water flow between horizontal parallel plates with asymmetric heating, over the range of Grashof number $4.3 \times 10^5 \leq Gr \leq 4.2 \times 10^8$ and Rayliegh number $65 \leq Ra \leq 1300$.

Experiments have been performed by Maughan and Incropera [7] to investigate mixed convection heat transfer in the thermal entrance region of a parallel plate channel heated from below. The effect of surface heat flux and channel orientation are studied for fluids at $Pr = 0.7$, and of Reynolds number $125 < Re < 500$, Grashof number $7 \times 10^3 < Gr < 1 \times 10^6$ and the inclination angle $0 \leq \theta \leq 30$.

Cheng, Kuan and Rosenberger [8] experimentally investigated the entrance effects of mixed convection between horizontal parallel plates heated from blew and cooled from above in the range of Rayliegh and Reynolds numbers $1368 < Ra < 8300$ and $15 < Re < 170$ for an aspect ratio of about 10.

Lee and Hwang [9] numerically studied the effect of asymmetric heating on the thermal instability in the thermal entrance region

of a parallel plate channel. Six different heating configurations are studied.
Nguyen [10] numerically studied mixed convection in the entrance region of a parallel plate channel at low Reynolds number employing the finite difference method. Correlations are obtained for the fully developed Nusselt number, hydrodynamic entrance length, thermal entrance length and the pressure drop.

2 Mathematical Description Of The Problem

As seen in figure (1), consideration is given to two horizontal parallel plates aligned parallel to a steady laminar flow and subjected to either symmetric or asymmetric constant wall temperatures. A cartesian coordinate system is used with the origin at the leading edge of the bottom plate. The free stream velocity at the inlet, temperature, and density at the center line are denoted by u_o ,T_o and ρ_o respectively. The velocity components in the longitudinal and transverse directions are denoted by u and v, respectively, while the vertical distance between the lower and upper plates is denoted by b. According to the Boussnisq approximation, the physical properties of the fluid are assumed to be constant except for the density ρ in the buoyancy term.
The flow and heat transfer process of the problem under investigation can be described by the following equations;

$$\partial u/\partial x + \partial v/\partial y = 0, \qquad (1)$$

$$u\,(\partial u/\partial x) + v(\partial u/\partial y) = -(1/\rho_o)\,\partial p/\partial x + \nu\,(\partial^2 u/\partial y^2) \qquad (2)$$

$$(\partial p/\partial y) = g\,(\rho_o - \rho), \qquad (3)$$

$$\beta = -(1/\rho_o)\,(\partial \rho/\partial T)_p \qquad (4)$$

$$u(\partial T/\partial x) + v(\partial T/\partial y) = k/\rho_o c_p\,(\partial^2 T/\partial y^2) \qquad (5)$$

THe following boundary conditions are applied;

$$u = v = 0\,, \quad T = T_w \quad \text{at } y = 0,\ b$$

$$u = u_{o,x}\,, \quad T = T_o\,, \quad \partial T/\partial y = 0 \quad \text{at } y = b/2\,. \qquad (6)$$

where $u_{o,x}$, is the velocity at the axis of the passage at any position x. In the system of equations (1-5) the term $(\rho-\rho)_o$ in equation (3) is eliminated in favor of the temperature difference $(T-T_o)$ through the definition of the coefficient of thermal expansion β, then the two equations of motion are cross differentiated and subtracted to eliminate the pressure gradient.

The governing equations become;

$$u\frac{\partial^2 u}{\partial x \partial y} + v\frac{\partial^2 u}{\partial y^2} - \nu\frac{\partial^3 u}{\partial y^3} + g\beta\frac{\partial}{\partial x}(T-T_o) = 0 , \qquad (7)$$

$$u\frac{\partial T}{\partial x} + v\frac{\partial T}{\partial y} = \frac{k}{\rho_o c_p}\left(\frac{\partial^2 T}{\partial y^2}\right), \qquad (8)$$

In the method of solution of the system of equations (7 and 8), one expresses these equations in a dimensionless form by defining new dimensionless independent variables, $\xi(x)$ and $\eta(x,y)$ along with a dimensionless temperature ϑ and a dimensionless stream function ψ, ccording to,

$$\xi(x) = Gr_x/Re_x^{5/2} \quad ; \quad \eta(x,y) = y\sqrt{u_o/\nu.x} , \qquad (9)$$

$$\psi = f(\xi,\eta)\sqrt{u_o\ \nu\ x} \quad ; \quad \vartheta = Tr\ [(T-T_o)/(T_l-T_o)], \qquad (10)$$

where; T_l and T_u are the lower and upper plate temperatures, respectively .The coefficient Tr is defined through the following relations as,

$$Tr = \frac{(2\phi + 1)\ \phi}{(2+\phi)} \quad ; \quad \phi = (T_l-T_o)/(T_u-T_o) \qquad (11)$$

It is noteworthy that both ϕ and Tr are so formulated that they ensure smooth transition between the different heating conditions. Using the foregoing definitions of the dimensionless dependent and independent variables (9-11) one can obtain the dimensionless form of the governing equations as;

$$2f''' + ff'' + \xi/Tr\ \eta\vartheta =$$

$$-\xi\left(f'\frac{\partial f'}{\partial \xi} - f''\frac{\partial f}{\partial \xi} + \xi/Tr\ \frac{\partial \vartheta}{\partial \xi}\right) , \qquad (12)$$

$$\frac{2}{Pr}\vartheta'' + f\vartheta' = \xi\left(f'\frac{\partial \vartheta}{\partial \xi} - \vartheta'\frac{\partial f}{\partial \xi}\right) , \qquad (13)$$

with the boundary conditions ;

$$f(\xi,0)=f'(\xi,0) = 0 \quad , \vartheta(\xi,0) = 1,$$
$$f(\xi,\eta_{b/2}) = \vartheta(\xi,\eta_{b/2}) = 0 \quad ,$$
$$f(\xi,\eta_b)=f'(\xi,\eta_b)= 0 \quad , \vartheta(\xi,\eta_b) = 1 \qquad (14)$$

where the primes denote partial differentiation with respect to η. The dimensionless variable $\eta_{b/2}$ appears in the boundary conditions is the value of the independent variable η corresponding to y=b/2 ,i.e., at the axis of the passage. Accordingly, with the aid of equation (9), the definition of $\eta_{b/2}$ can be deduced as,

$$\eta_{b/2} = \xi_b/\xi \ , \qquad (15)$$

where,

$$\xi_b = Gr_b/2\ Re_b^2 = [g\beta(T_l-T_o)/2u_o^2].b \qquad (16)$$

From equation (16) , it is seen that the configuration parameter ξ_b is directly proportional to the height of the passage. Obtaining the velocity and temperature profiles, the physical quantities of interest, namely, the local Nusselt number and the local coefficient of friction can now be deduced.
Defining the local Nusselt number and the local coefficient of friction as;

$$Nu_x = hx/k \ , \qquad C_f = \tau_w/(\rho u_o^2) \tag{17}$$

where

$$h=q_w/(\Delta T_1-\Delta T_2)=-k\ [(\partial T/\partial y)_{y=0}+(\partial T/\partial y)_{y=b}] \ , \tag{18}$$

$$\tau_w=\rho\nu(\partial u/\partial y)_{y=0} \ , \ \Delta T_1=(T_l-T_o), \quad \Delta T_2=(T_u-T_o) \tag{19}$$

Employing the definitions of f and ϑ and their derivatives, one can express the local Nusselt number and the local coefficient of friction in a dimensionless form as;

$$Nu_x/\sqrt{Re_x} = (\vartheta_l' + \vartheta_u') \frac{\phi}{Tr(1+\phi)} \ . \tag{20}$$

$$C_f \sqrt{Re_x} = f''(\xi,0). \tag{21}$$

Nusselt number can also be presented in the conventional form as,

$$Nu_b = 2\eta_{max} (\vartheta_l' + \vartheta_u') \left(\frac{\phi}{Tr(1\pm\phi)}\right). \tag{22}$$

The method of the local similarity solutions is adopted to simplify the governing equations by divesting them from the terms causing nonsimilarity, this is based on the assumption that variations in f and ϑ and their derivatives with respect to ξ is much smaller than that with respect to η. In this sense the terms containing $\frac{\partial \Sigma}{\partial \xi}$ in equations (12 and 13) are considered comparatively small and the right hand sides in these equations vanish. This approximation is fairly justifiable for sufficiently small values of ξ where the quantities $\xi\frac{\partial}{\partial \xi}$ and $\xi^2\frac{\partial}{\partial \xi}$ are very small. Based on the above mentioned postulate, the momentum and energy equations will be reduced to,

$$f'''' + 1/2 f f''' + 1/2 f f''' + 1/2 \ \xi/Tr \ \eta \ \vartheta' = 0, \tag{23}$$

$$\vartheta'' + 1/2 \ Pr \ f \ \vartheta' = 0. \tag{24}$$

Furthermore the momentum equation (23) can be directly integrated with respect to η with the result that the set of equations governing the problem becomes,

$$f''' + 1/2 \ ff'' + 1/2 \ \xi/Tr \ . \eta\vartheta + 1/2 \ \xi/Tr \int \vartheta \ d\eta = 0 \ , \tag{25}$$

$$\theta'' + 1/2\ Pr\ f\ \theta' = 0\ , \qquad (26)$$

with the boundary conditions.

$$f(\xi,0) = f'(\xi,0) = 0\ , \qquad \theta(\xi,0) = Tr\ ,$$
$$f(\xi,\eta_b) = f'(\xi,\eta_b) = 0\ ,$$
$$\theta(\xi,\eta_b) = Tr\ \phi \qquad (27)$$

It is seen that the boundary conditions associated with equations (25 and 26) are insufficient to determine a solution. The present method of solution entails dividing the flow field into two imaginary parts, one of which encloses the region from the lower wall to the axis of the passage and the other encloses the region from the upper wall to the axis of the passage. Furthermore, the continuity equation in the integral form is employed to provide criteria for the calculation of the correct velocity profile as follows;

$$\eta_{b/2} = \int_0^{\eta_{b/2}} f'\, d\eta . \qquad (28)$$

The boundary conditions along with equation (28) are now quite sufficient to determine local solutions regrading ξ as a constant parameter at any axial position.

Numerical Solution

The basic algorithm for the approximate solution of such a problem involves guessing the unknown values of $f''(\xi,0)$ and $\theta'(\xi,0)$ and integrate the governing equations across the specified interval to obtain approximate solution to the problem which depends upon the initially guessed values of $f''(\xi,0)$ and $\theta'(\xi,0)$. If the required outer boundary conditions are satisfied, a solution has been obtained, otherwise an iterative shooting method is employed to estimate new improved values for both $f''(\xi,0)$ and $\theta'(\xi,0)$ for the next trial integration. However the problem is further complicated by the fact that the value of f' at the outer boundary, i.e., $f'(\xi,\eta_{b/2})$ is also unknown, which introduces another initial guess to the input data; that has also to be corrected by adjusting the produced velocity profile to satisfy the continuity equation in the integral form this process is repeated several times until satisfactory results are achieved.

The numerical scheme designed to execute the foregoing sequence of steps employs both the Runge-Kutta method of the ordinary differential equations as an integration technique and the Newton-Raphson iterative method to carry out the successive improvements according to the shooting method. Each of the configuration parameter ξ_b, the temperature ratio ϕ and Prandtl number Pr are varied over the whole range of the mixed convection parameter ξ. In the solution of the upper half of the passage, the

sign of the buoyancy term in the momentum equation is changed to negative to account for the positive pressure gradient associated with the flow below a heated surface.

4. RESULTS AND DISCUSSION

Numerical calculations are carried out over the range of the mixed convection parameter $0.0 \leq \xi \leq 0.$ for Prandtl number values of 0.7, 2 and 5 . The configuration parameter ξ_b is varied between 0.3 to 0.5 , while the temperature ratio ϕ is assigned the values 1, 2 and 3.

Figures (2 and 3) repreesent the effect of the mixed convection parameter, ξ on the velocity and temperature profiles for $\phi = 2$, Pr = 0.7 and $\xi_b = 0.4$. Buoyancy effects are seen to profoundly distort the velocity profile which exhibited an overshoot beyond the free stream limit in the lower half of the passage. Such distortion in the velocity is much less pronounced in the upper half of the passage. This may be due to the opposing pressure gradient which has hysteresis behavior on the velocity development.

Results reveal also that, large temperature gradients are associated with higher values of the mixed convection parameter ξ, this in turn leads to heat transfer enhancement.

Variation of both the local heat transfer expressed as $Nu_x/\sqrt{Re_x}$ and $Nu_b=(hb/k)$ are depicted in figures (4 and 5) as functions of the mixed convection parameter ξ which varies over the range $0.018 \leq \xi \leq 0.1$. Results are obtained for values of the configuration parameter, ξ_b, of 0.3, 0.4 and 0.5.

Figure (4) indicates remarkable enhancement in the local heat transfer $(Nu_x/\sqrt{Re_x})$ as ξ_b decreases, this is due to the large temperature gradients at the walls associated with the lower values of ξ_b. In figure (5) this trend is reversed with higher values of ξ_b leads to higher values of Nu_b

Results of the effect of ξ_b on the coefficient of friction is presented in figure (6). It is seen that curves of lower values of ξ_b lie above those of higher values and become much more steep as the mixed convection parameter increases.

Effect of Prandtl number on Nusselt number and the wall shear stress is depicted in figures (7 and 9) over the range $0.022 \leq \xi \leq 0.1$. Values of Prandtl number are taken as 0.7, 2 and 5. An enhancement in both the coefficient of friction and Nusselt number is seen associated with higher values of Prandtl number.

The temperature ratio, ϕ seems to have an effect similar to that of Prandtl number on the velocity and temperature profiles as shown in figures (8-9). The relatively strong effect of both the temperature

ratio and Prandtl number on the temperature profile is probably due to the direct effect of these two factors on the energy equation.
In figures (10-11) results reveal decreased heat transfer enhancement with lower values of the temperature ratio ϕ. Such behavior is an excepected consequence of the effect that the increasing top heating has on the core fluid, since by decreasing ϕ, the temperature of the fluid at the core region increases and its ability of cooling the bottom plate diminishes. Closer inspection of the two figures may confirm this explanation, since, as the distance from the leading edge increases the core fluid becomes already warmed, and the wall-minus-free stream temperature difference approaches a constant value,at this limit , the difference between the curves of different ϕ's seems to vanish to zero.
The effect of the temperature ratio, ϕ on the local coefficient of friction is presented in figure (12) as a function of the mixed convection parameter ξ. Solutions are obtained over the range $0.014 \le \xi \le 0.06$ The figure indicates that, the coefficient of skin friction ($C_f\sqrt{Re_x}$) increases as ϕ increases due to the large velocity gradients associated with the higher values of the temperature ratio.

5. CONCLUSIONS

With the appropriate dimensionless transformation of the governing equations, the method of the local similarity solutions could be used to simplify these equations to a system of ordinary differential equations. The problem was simplified to the simultaneous solution of two flat plates and the continuity equation in the integral form was used to match the two solution at the center of the passage. This method is simple and self starting. Contrasting the obtained results with the previous studies of Abu-Ellial et al [4] Osborne et al [7] and Morcos et al [9] (figures 13-15) evidences the reliability of the present method.

REFERENCES

[1] Cheng, K.C., and G.J.Hwang. Numerical Solution For Combined Forced And Free Laminar Convection In Horizontal Rectangular Channels, Transactions of the ASME, Vol. 91, PP. 59-66, 1969.
[2] Hwang, G.J.,and Cheng, K.C., Convective Insatiability In The Thermal Entrance Region Of a Horizontal Parallel Plate Channel Heated From Below, Transactions Of The ASME, Vol. 95, PP. 72-77, 1973.
[3] Wuu-Ou, J., Cheng, K.C.,and Lin, R.C.,Combined Free And Forced Laminar Convection In Inclined Rectangular Channels, Int. J. Of Heat Mass Transfer, Vol. 19, PP. 277-183, 1976.
[4] Abu-Ellail, M.M., and Morcos, S.M.,Buoyancy Effects In The Entrance Region Of Horizontal Rectangular Channels, Transactions Of The ASME, Vol. 105, PP. 924-927, 1983.

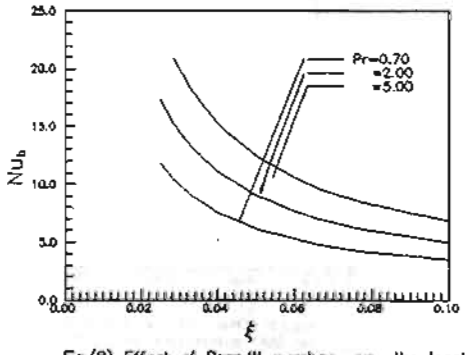

Fig.(8) Effect of Prandtl number on the local Nusselt number for ξ_b=0.5, φ=2.0

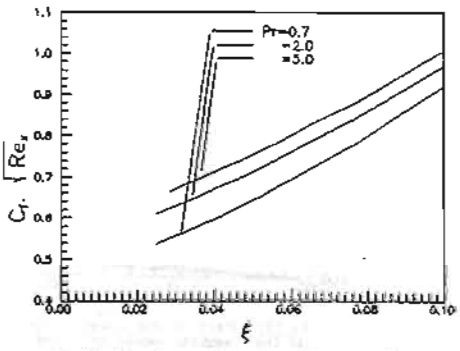

Fig.(9) Effect of Prandtl number on the coefficient of friction for φ=2.0, ξ_b=0.5

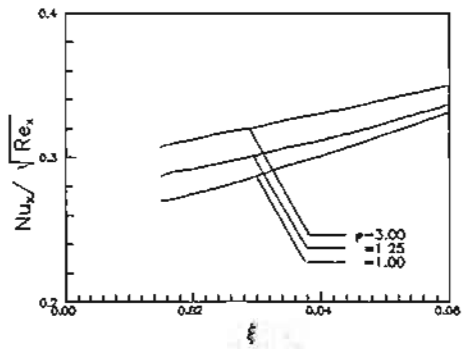

Fig. (10) Effect of the temperature ratio, φ on Nusselt number for ξ_b=0.3, Pr=0.7

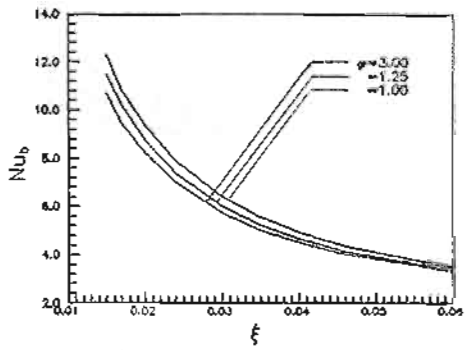

Fig.(11) Effect of the temperature ratio, φ on the local Nusselt number for ξ_b=0.3, Pr=0.7

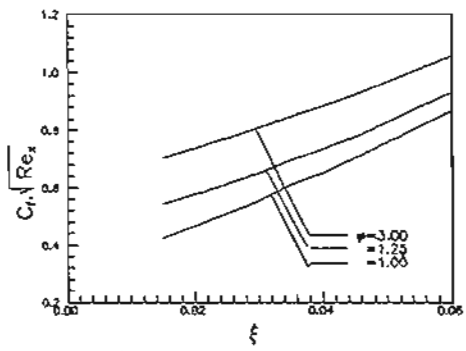

Fig.(12) effect of the temperature ratio, φ on the coefficient of friction for ξ_b=0.3, Pr=0.7